

# FOUR-PHOTON CORRECTION IN TWO-PHOTON BELL EXPERIMENTS

Valerio Scarani, Hugues de Riedmatten, Ivan Marcikic, Hugo Zbinden, Nicolas Gisin

Group of Applied Physics, University of Geneva

20, rue de l'Ecole-de-Médecine, CH-1211 Geneva 4, Switzerland

October 23, 2018

## Abstract

Correlated photons produced by spontaneous parametric down-conversion are an essential tool for quantum communication, especially suited for long-distance connections. To have a reasonable count rate after all the losses in the propagation and the filters needed to improve the coherence, it is convenient to increase the intensity of the laser that pumps the non-linear crystal. By doing so, however, the importance of the four-photon component of the down-converted field increases, thus degrading the quality of two-photon interferences. In this paper, we present an easy derivation of this nuisance valid for any form of entanglement generated by down-conversion, followed by a full study of the problem for time-bin entanglement. We find that the visibility of two-photon interferences decreases as  $V = 1 - 2\rho$ , where  $\rho$  is, in usual situations, the probability per pulse of creating a detectable photon pair. In particular, the decrease of  $V$  is independent of the coherence of the four-photon term. Thanks to the fact that  $\rho$  can be measured independently of  $V$ , the experimental verification of our prediction is provided for two different configuration of filters.

## 1 Introduction

The distribution of a pair of entangled photons to two distant partners is the building block of quantum communication protocols [1, 2]. The entangled photons are produced by parametric down-conversion (PDC) in a non-linear crystal. As well-known, this process creates pairs of photons at the first order; but when the pumping intensity increases, four- and more-photon components become important in the down-converted field [3, 4]. If one can post-select the number of photons, higher-photon components of the field may turn out to be a useful resource (an "entanglement laser", see [5]). In other cases however, these higher-number components turn out to be quite a nuisance. In particular, one is often interested in two-photon phenomena, just think of the Bell-state measurement (BSM) that is needed in teleportation. The presence of higher-number components obviously degrades the quality of the two-photon interferences. In long-distance implementations, one can hardly overcome this nuisance by working with low pump intensities: after propagation along several kilometers of fibers, many photons are lost because of the losses in the fibers, and the efficiency of the detectors at telecom wavelengths is low, typically 10%. Moreover, if the two photons

come from different sources and have to interfere at a beam-splitter (as is the case for the BSM), filters must be introduced to ensure coherence. Thus, in order to have a reasonable count rate, one has to increase the pump power — and this unavoidably increases the number of unwanted higher-number components. In this paper, we address the degradation of the visibility of two-photon interferences due to the presence of four-photon components in the field, thus completing the partial study provided in Ref. [6].

In Section 2, we give an easy derivation of the topic and the results that is valid for any form of entanglement generated by down-conversion, under the assumption that the four-photon component is described by two independent pairs. In the rest of the paper, we relax that assumption: indeed, the four-photon coherence can vary from zero (two independent pairs) to one (state of single-mode down-conversion [7]) according to the experimental conditions [8, 9, 10]. We prove that the loss of visibility does not depend on the coherence of the four-photon state, but only on a parameter  $\rho$  that is basically the probability of creating a detectable pair. For this full study, we shall focus on *time-bin entanglement*, a form of entanglement that is more robust than polarization for long-distance applications in optical fibers. Visibilities large enough to allow the violation of Bell's inequalities for two photon [6, 11], quantum cryptography [12], and long-distance teleportation [13] have been demonstrated in the recent years for this form of entanglement. For time-bin entanglement, the present study requires the multimode formalism, introduced in Section 3. In fact, as the name suggests, a time-bin qubit is a coherent superposition of two orthogonal possibilities, the photon being at a given time  $t = 0$  (first time-bin) or at a later time  $t = \tau$  (second time-bin). Separate time-bins must be created by a pump field consisting of separate pulses: the finite temporal size (thence, the non-monochromaticity) of the pump pulses and the down-converted photons is a necessary feature of time-bin qubits.

In Section 4, we describe a setup that is used for measure the parameter  $\rho$ . In Section 5, we introduce the setup for measuring time-bin entanglement (a Franson interferometer with a suitable source) and derive our main prediction, namely the decrease of visibility due to the presence of four-photon components in the state. In Section 6 we describe the experimental verification of our predictions. Section 7 is a conclusion. For readability, the technicalities of the formalism used in Sections 4 and 5 are left for an Appendix. We note that the calculations of the two-photon coincidence rate provides the first explicit calculation of time-bin Bell experiments using the full formalism of quantum optics.

## 2 Easy derivation for incoherent four-photon component

The purpose of this Section is to derive the main results from a simple formalism, in order to gain intuition about the physics of the problem. The content of this Section does not apply only to time-bin entanglement, but to any form of entanglement obtained by down-conversion, be it with a cw or with a pulsed pump laser. The probabilities that we are going to introduce in this Section are "per detection window". In the case of a cw pump, this means "per time resolution of the detector"; in the case of a pulsed pump, this means "per pump pulse" ("per qubit", in the language of time-bin entanglement [14]).

The calculation is possible in simple terms if we neglect the coherence of the four-photon term, and assume that when four photons are produced, they form two independent pairs. The process of creation of indepen-

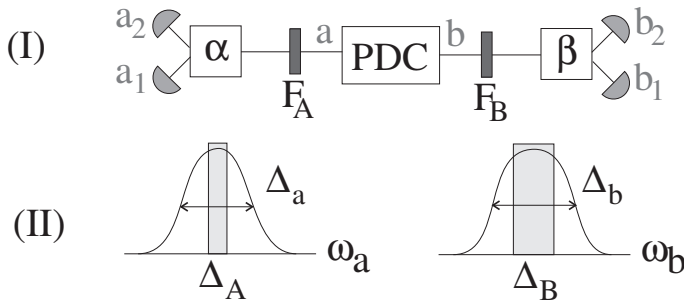


Figure 1: (I) Experimental setup to measure two-photon interferences, and meaningful parameters. Grey letters: spatial modes in the fibers; PDC: parametric down-conversions; F: filters. (II) Spectral widths of the down-converted photons (curves) and filters (grey shadows). Both filters are centered in the spectrum of the down-converted photons, and their width are  $\Delta_A \leq \Delta_B$ .

dent items obeys the Poissonian statistics: if  $P_{2c}$  is the probability of creating a pair, we have  $P_{4c} \simeq \frac{1}{2}P_{2c}^2$ . For the setup, we refer to Fig. 1. We define  $\Delta_{a,b}$  as the spectral width of the photons in mode  $a$ , resp.  $b$ , after down-conversion, that is, before the filters; the spectral width of the pump is denoted  $\Delta_p$ . As for the filters, we suppose that they are centered in the spectrum of the down-converted photons, and that they satisfy  $\Delta_{A,B} \leq \Delta_{a,b}$  to avoid trivialities; furthermore, we suppose  $\Delta_{A,B} \gg \Delta_p$ , so that twin photons certainly pass both filters, and  $\Delta_B \geq \Delta_A$ . Let's follow the two- and the four-photon component through the setup, until the coincidence detection in modes  $a_1$  and  $b_1$ .

*Two-photon component.* To have a detection, both photons must pass the filters; because of the correlation in energy, if photon  $a$  passes through  $F_A$  (that happens with probability  $\sim \Delta_A/\Delta_a$ ), then certainly photon  $b$  will pass through  $F_B$ , because this filter is larger and the photons are correlated in energy. The photons are twins, therefore they interfere. Consequently, the detection rate due to two-photon components is (up to multiplicative factors)

$$R_2 = P_{2c} \frac{\Delta_A}{\Delta_a} \frac{1}{2} [1 + \cos(\alpha + \beta)]. \quad (1)$$

*Four-photon component.* Once four photons have been produced, four two-photon coincidence events are possible: two events in which we detect photons belonging to the same pair, and two events in which we detect photons belonging to different pairs. The first case is similar to the case of two-photons. In the second case, however, the fact that photon  $a$  passes its filter does not guarantee at all that photon  $b$  will do it as well; and of course, no interference will take place. All in all,

$$R_4 = P_{4c} \left\{ 2 \frac{\Delta_A}{\Delta_a} \frac{1}{2} [1 + \cos(\alpha + \beta)] + 2 \frac{\Delta_A}{\Delta_a} \frac{\Delta_B}{\Delta_b} \frac{1}{2} \right\}. \quad (2)$$

The total count rate is therefore  $R_2 + R_4 = \bar{R} \frac{1}{2} [1 + V \cos(\alpha + \beta)]$  where  $\bar{R} \simeq P_{2c} \frac{\Delta_A}{\Delta_a}$  and where the visibility  $V$  is

$$V = \frac{1}{1 + \frac{P_{2c}}{1+P_{2c}} \frac{\Delta_B}{\Delta_b}} = 1 - P_{2c} \frac{\Delta_B}{\Delta_b} + O(P_{2c}^2). \quad (3)$$

Recall that  $\Delta_B$  is singled out by the relation  $\Delta_B \geq \Delta_A$ . As expected,  $V$  decreases if  $P_{2c}$  (proportional to the pump power) is increased. Note also that  $\frac{\Delta_B}{\Delta_b} \leq 1$ : for a given pump power, the visibility increases if filters are in place. This is intuitive, considering the emission of two pairs: conditioned to the fact that photon in mode  $a$  has passed the filter  $F_A$ , a photon passing  $F_B$  is more likely to be its twin (whose frequency *must* lie within the filter) than an uncorrelated photon (whose frequency may lie everywhere in the spectrum). Finally, if only one filter is in place, then  $\frac{\Delta_B}{\Delta_b} = 1$  and we recover the discussion presented in Ref. [6].

However, we are not really interested in fixing the pump power: rather, we'd like to fix the coincidence rate at the detection  $\bar{R}$ . Obviously, this means that if we narrow the filters, we must increase the pump power in order to keep the coincidence rate constant. Strictly speaking, the quantity  $P_{2c} \frac{\Delta_B}{\Delta_b}$  is the probability per qubit of creating a photon pair such that the photon in mode  $b$  passes through the (larger) filter. However,  $\frac{\Delta_A}{\Delta_a} \simeq \frac{\Delta_B}{\Delta_b}$  holds in magnitude for typical down-conversion processes and filters; consequently,  $P_{2c} \frac{\Delta_B}{\Delta_b} \simeq \bar{R}$  is an estimate of the probability of creating a detectable pair.

The results of this Section are based on the assumption that the four-photon state is always described by two independent pairs. Note that this assumption is certainly good in the case of cw pump, because the time resolution of the detector is much larger than the coherence time of the down-converted photons. The assumption is more questionable in the case of a pulsed pump. The rest of the paper shows, focusing specifically on time-bin entanglement, that the degradation of visibility (3) is actually independent of the coherence of the four-photon term.

### 3 General approach

#### 3.1 The state out of down-conversion

The formalism to describe multimode down-conversion was introduced in Refs [15, 16] for the two-photon component, and extended to the four-photon component for type-I down-conversion in [17]. We have applied this formalism to our case in Ref. [9]; we summarize here the main notations and results.

The pump field is assumed to be classical, composed of two identical but delayed pulses:  $P(t) = \sqrt{I_p} (p(t) + p(t + \tau))$ , so in Fourier space

$$\tilde{P}(\omega) = \sqrt{I_p} \tilde{p}(\omega) (1 + e^{i\omega\tau}) . \quad (4)$$

We use colinear type-I down-conversion in a non-degenerate regime  $\omega_s \neq \omega_i$ ; therefore, the signal and the idler photons can be coupled into different spatial modes  $a$  and  $b$  using a wavelength division multiplexer (WDM). The phase-matching function is written  $\Phi(\omega_a, \omega_b)$ ; we don't need its explicit form in what follows. For convenience we define the following notations:

$$\Phi(x, y) \tilde{p}(x + y) (1 + e^{i(x+y)\tau}) \equiv g(x, y) (1 + e^{i(x+y)\tau}) \equiv G(x, y) . \quad (5)$$

The state produced by the down-conversion in the crystal reads

$$|\Psi\rangle = i\sqrt{I} \mathcal{A}^\dagger |vac\rangle + \frac{I}{2} (\mathcal{A}^\dagger)^2 |vac\rangle + O(I^{3/2}) \quad (6)$$

where  $I$  is proportional to the intensity  $I_p$  of the pump, and

$$\mathcal{A}^\dagger = \int d\omega_a d\omega_b G(\omega_a, \omega_b) a^\dagger(\omega_a) b^\dagger(\omega_b). \quad (7)$$

### 3.2 Detection: generalities

We have just given the state  $|\Psi\rangle$  created by down-conversion. This state evolves through the setup (in our case, a linear optics one so that the number of photons is conserved) according to  $|\Psi\rangle \rightarrow |\hat{\Psi}\rangle$ , then two-photon coincidences are recorded. Here we introduce the general scheme for this detection. Let's write  $a_1$  and  $b_1$  the spatial modes on which one looks for coincidences; since no ambiguity is possibly, we write  $a_1$  and  $b_1$  also the corresponding annihilation operators. We look at detector on mode  $a_1$  at time  $T_A \pm \Delta T$ , where  $\Delta T$  is the time resolution of the detectors; similarly for detection on mode  $b_1$ . The coincidence rate reads

$$R(T_A, T_B) = \eta_A \eta_B \int_{T_A - \Delta T}^{T_A + \Delta T} dt_A \int_{T_B - \Delta T}^{T_B + \Delta T} dt_B \|E_{a_1}^{(+)}(t_A) E_{b_1}^{(+)}(t_B) |\hat{\Psi}\rangle\|^2. \quad (8)$$

In this formula,  $\eta_{A,B}$  are constant factors [18] that will be omitted in all that follows; the positive part of the electric field on mode  $a_1$  is defined as

$$E_{a_1}^{(+)}(t) = \int d\nu f_A(\nu) e^{-i\nu t} a_1(\nu). \quad (9)$$

with  $f_A(\nu)$  is a real function describing a filter in mode  $a_1$ , the transmission of the filter being  $F_A(\nu) = f_A(\nu)^2$ . The definition of  $E_{b_1}^{(+)}(t)$  is analogous. We choose the origin of times in order to remove the free propagation from the crystal to the detectors. Therefore, the first time-bin at the detection is given by  $t_j = 0$ , the second time-bin by  $t_j = \tau$  and so on.

Actually, formula (8) for detection is exact for proportional counters, in which the probability of detection is the intensity of the field. For photon counting with a detector of quantum efficiency  $\eta$ , the probability of the detector firing, given that  $n$  photons imping on it, is not  $n\eta$  (proportional to the intensity) but  $(1 - (1 - \eta)^n)$ . Now, for the wavelengths that we consider, the quantum efficiency is  $\eta \approx 0.1$ ; moreover, the mean number of photons that imping on a detector is much smaller than 1 because of the losses in the fibers and in the coupling; finally, in our formalism we restrict to the four-photon term, so that at most two photons can imping on the detector. All in all, the approximation  $(1 - (1 - \eta)^2) \simeq 2\eta$  holds and we can indeed use (8) to compute the coincidence rate.

### 3.3 Important parameters

As we said in the introduction, we shall postpone the detailed calculations to the Appendix. All the results of the Sections 4 and 5 can be formulated using the following parameters: writing  $d\underline{\omega} = d\omega_a d\omega_b$ ,

$$J = \int d\underline{\omega} |g(\omega_a, \omega_b)|^2, \quad (10)$$

$$J_A = \int d\underline{\omega} F_A(\omega_a) |g(\omega_a, \omega_b)|^2 \quad (11)$$

$$J_B = \int d\underline{\omega} F_B(\omega_b) |g(\omega_a, \omega_b)|^2 \quad (12)$$

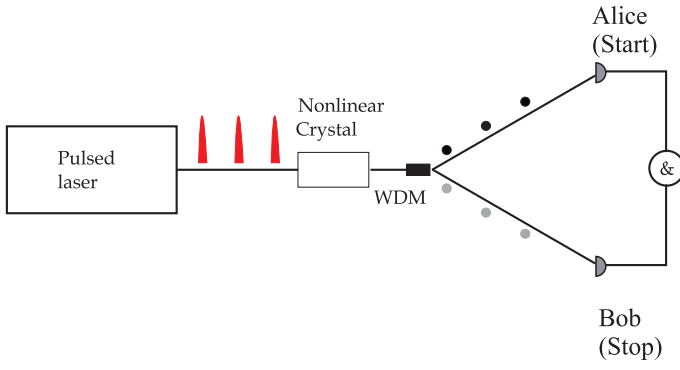


Figure 2: Schematic of the setup used to measure the parameter  $\rho$ .

$$J_{AB} = \int d\underline{\omega} F_A(\omega_a) F_B(\omega_b) |g(\omega_a, \omega_b)|^2, \quad (13)$$

$$J_4 = \int d\underline{\omega} d\underline{\omega}' F_A(\omega_a) F_B(\omega_b) [g^*(\omega_a, \omega_b) g^*(\omega'_a, \omega'_b) g(\omega_a, \omega'_b) g(\omega'_a, \omega_b) + c.c.] , \quad (14)$$

The first four numbers can be given an intuitive meaning. In fact, up to multiplicative factors:  $J$  is the probability of producing two photons in one pump pulse, irrespective of whether they will pass the filter or not;  $J_A$  and  $J_B$  are the probabilities of producing two photons in one pump pulse, and that the photon in mode  $a$  (resp.  $b$ ) passes through the filter;  $J_{AB}$  is the probability of producing two photons in one pump pulse and both photons pass the filter. The interpretation of  $J_4$  is somehow more involved: it is a coherence term, due to the fact that the four photon state cannot be described as two independent pairs [9].

Obviously,  $J_{AB} = J_A$  if no filter is applied on B. But  $J_{AB} = J_A$  holds to a very good approximation also if  $\Delta_A < \Delta_B$ , where  $\Delta_X$  is the width of filter  $F_X$ , provided that both filters are larger than the spectral width of the pump  $\Delta_p$  (as we supposed in Section 2, and as will be the case in the experiment). In fact, in this case, detection of a photon in filter A automatically ensures that its twin photon has a frequency within the range of filter B, which means  $F_B(\omega_b) = 1$  for all  $\omega_b$  compatible with the phase-matching condition.

## 4 A calibration setup

Before describing the measurement of two-photon interferences (next Section) we present an experimental setup that allows to measure the probability  $\rho$  of creating a detectable pair in a simple way. This setup (see Fig. 2) has been presented in detail in section IV of Ref. [6]. We give here a brief description. A Fourier-transform-limited pulsed laser is used to create non-degenerate photon pairs at telecommunication wavelengths (1310 and 1550 nm) by parametric down-conversion in a non linear-crystal. The two photons are separated deterministically using a wavelength-division multiplexer (WDM) and each photon is detected by single-photon counters (avalanche photodiodes). The signal from the two detectors are then sent to a Time-to-Digital converter, which is used to determine the histogram of the differences in the time of arrival of the twin photons.

We apply our formalism to this setup. For the detection, since there is no evolution but the free propagation, we have simply  $a_1 = a$  and  $b_1 = b$ . For the preparation, at first sight it seems that our formalism should be modified: we are dealing with a train of  $N$  pulses instead of only two pulses, so  $(1 + e^{i\omega\tau})$  should be replaced with  $\sum_{k=0}^{N-1} e^{i\omega k\tau}$  in formula (4). However, a closer look shows that we can do the calculation without any change. In fact, in this particular setup there is no interference: then,  $R_C$  is simply the sum of the coincidence rates obtained when the two photons arrive at the same time, while  $R_L$  is the sum of the coincidence rates obtained when photon in mode  $a$  arrives a time  $\tau$  later than the photon in mode  $b$ . Since moreover  $R(k\tau, k\tau) = R(0, 0)$  and  $R((k+1)\tau, k\tau) = R(\tau, 0)$  for all  $k$ , we obtain  $R_C = N R(0, 0)$  and  $R_L = (N-1) R(\tau, 0)$ , so we can focus on only two successive pulses. By the way,  $R(0, 0)$  is proportional to the probability per pulse of creating one detectable pair (a pair that will pass the filters).

The calculation is given in the Appendix, and the results are  $R(0, 0) = I J_{AB} + O(I^2)$  and  $R(\tau, 0) = I^2 J_A J_B$ , that are indeed what one expects because of the meaning of the  $J$ 's (subsection 3.3). Therefore, in the limit of large  $N$ , the ratio  $\rho$  between the integrals of the side peak and the central peak is

$$\rho = I \frac{J_A J_B}{J_{AB}}. \quad (15)$$

In most cases,  $\rho$  has a simple interpretation. In fact, whenever condition  $\Delta_p \ll \Delta_A < \Delta_B$  holds, we have seen above that  $J_{AB} = J_A$  and consequently  $\rho = I J_B$  is the probability per pulse of creating a pair such that the photon that meets the largest filter will pass it. In particular, if there is no filter on mode  $b$ ,  $\rho$  is the probability per pulse of creating a pair, as noticed in the Appendix of [6]. That derivation shares with the present one the hypothesis of small detector efficiency, but is otherwise rather different: in our previous paper, we supposed that a  $2N$ -photon state is actually  $N$  independent pairs; here, we limit ourselves to 2 and 4 photons, but derive the result without any assumption about the coherence of the 4-photon state. Moreover, as argued in Section 2, since  $J_A \simeq J_B$  normally holds, at least in magnitude, then  $\rho \simeq I J_A = R(0, 0)$  is an estimate of the probability per pulse of creating a detectable pair.

## 5 The Franson interferometer

### 5.1 Description of the setup

We turn now to the main setup, which is the interferometer that allows the analysis of time-bin entanglement (see Fig.3). This is essentially the interferometer proposed by Franson to study energy-time entanglement [19], completed with an unbalanced interferometer before the crystal (the pump interferometer). A laser pulse is first split in two in this interferometer. At its exit, we have two laser pulses with a fixed phase difference separated by a time  $\tau$  corresponding to the path length difference between the long and the short arm of the interferometer. In the non linear crystal, we therefore create a photon pair in a coherent superposition of two time-bins.

After the crystal, the photons are separated with the WDM and each sent to a fiber interferometer in order to make a two photon interference experiment.

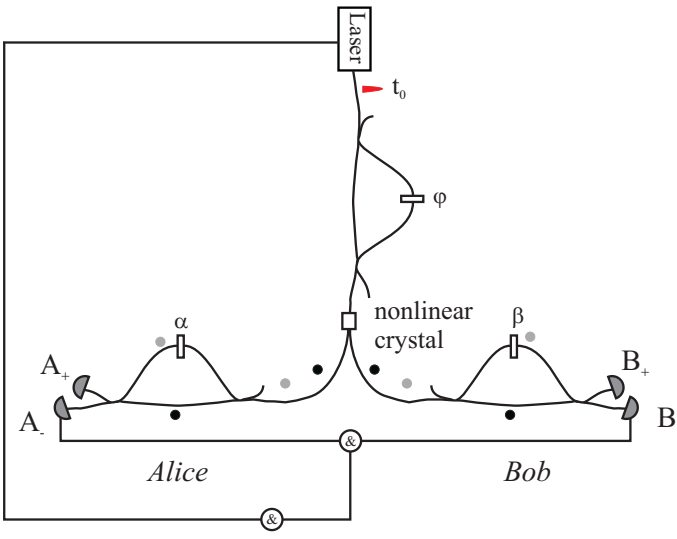


Figure 3: Schematic of the setup used to measure two photon quantum interference with time-bin entangled qubits. In addition to the two-photon coincidence, a coincidence with the pump laser provides the origin of time needed to define the three time-bins.

## 5.2 Evolution

The evolution of modes  $a$  and  $b$  in each arm of the interferometer is given by the following expressions:

$$a^\dagger(\omega) \longrightarrow \hat{a}^\dagger(\omega) = S(\omega, \alpha) a_1^\dagger(\omega) + C(\omega, \alpha) a_2^\dagger(\omega) \quad (16)$$

$$b^\dagger(\omega) \longrightarrow \hat{b}^\dagger(\omega) = S(\omega, \beta) b_1^\dagger(\omega) + C(\omega, \beta) b_2^\dagger(\omega) \quad (17)$$

with [20]

$$S(\omega, \theta) = \frac{1 - e^{i(\omega\tau + \theta)}}{2} \quad , \quad C(\omega, \theta) = i \frac{1 + e^{i(\omega\tau + \theta)}}{2} . \quad (18)$$

The evolved state  $|\hat{\Psi}\rangle$  is obtained by inserting the evolved operators  $\hat{a}^\dagger$  and  $\hat{b}^\dagger$  into  $|\Psi\rangle$ .

In these formulae, we have already supposed that the analyzing interferometers are identical to the pump interferometer. Thus, three time-bins are defined by the setup. The first time-bin,  $t = 0$ , corresponds to the time of arrival of photons produced by the first pump pulse and not delayed. The second or intermediate time-bin,  $t = \tau$ , corresponds to the time of arrival, either of photons produced by the first pump pulse and delayed, or of photons produced by the second pump pulse and not delayed. The third time-bin,  $t = 2\tau$ , corresponds to the time of arrival of photons produced by the second pump pulse and delayed. Interferences will only be seen when both photons arrive at  $t = \tau$ , because only in this case two indistinguishable alternatives are available.

## 5.3 Two-photon interferences

We study the detection for modes  $a_1$  and  $b_1$ ; all the other cases can be treated in the same way. The coincidence rate  $R(T_A, T_B)$  is the sum of two terms corresponding respectively to the two-photon and the



four-photon terms:

$$R_2(T_A, T_B) = I \int dt_A dt_B ||E_{a_1}^{(+)}(t_A) E_{b_1}^{(+)}(t_B) \hat{\mathcal{A}}^\dagger |vac\rangle||^2, \quad (19)$$

$$R_4(T_A, T_B) = \frac{I^2}{4} \int dt_A dt_B ||E_{a_1}^{(+)}(t_A) E_{b_1}^{(+)}(t_B) (\hat{\mathcal{A}}^\dagger)^2 |vac\rangle||^2. \quad (20)$$

Indeed, the two- and the four-photon states do not interfere (in principle, one could insert a non-destructive measurement of the number of photons just after the crystal, and this would not modify the rest of the experiment).

The calculation is presented in the Appendix. As said above, interferences will appear only in the intermediate time-bin  $T_A = T_B = \tau$ , in which case one finds [21]:

$$R_2(\tau, \tau) = I J_{AB} (1 + \cos(\alpha + \beta)), \quad (21)$$

$$R_4(\tau, \tau) = I^2 \left[ (2J_{AB}J + J_4) (1 + \cos(\alpha + \beta)) + 2J_A J_B \right]. \quad (22)$$

The result for  $R_2(\tau, \tau)$  is the expected one: one pair is produced, it passes the filters, and since it is in a superposition of being in both pulses it gives rise to full-visibility interferences. In the formula for  $R_4(\tau, \tau)$ , two contributions are also expected from the intuitive view of the four-photon state as two independent pairs: (i) the term containing  $J_{AB}J$  means that two pairs are created, the photons of the same pair are detected and therefore one has full visibility; (ii) the term containing  $J_A J_B$  means that two pairs are created, the photons of the different pair are detected and therefore they don't show any interference. The remarkable feature is the *position* of the correction due to the coherence in the four-photon term,  $J_4$ : it contributes to a full-visibility interference as well. This couldn't have been guessed without the full calculation.

Summing (21) and (22), the total two-photon coincidence rate in the intermediate time-bin reads

$$R(\tau, \tau) = R_2(\tau, \tau) + R_4(\tau, \tau) = \bar{R} [1 + V \cos(\alpha + \beta)] \quad (23)$$

where the average count rate  $\bar{R}$  is given by [21]

$$\bar{R} = I J_{AB} + O(I^2) \quad (24)$$

and the visibility  $V$  is given by  $V = \frac{1+I(J+J_4/J_{AB})}{1+I(J+(J_4+J_A J_B)/J_{AB})}$ . Now, the terms  $O(I^2)$  in the visibility are meaningless, because the six-photon term that we neglected completely contributes to the same order; so we have to keep only the first-order development of  $V$  in  $I$ , that leads to the remarkable relation

$$V \simeq 1 - I \frac{2J_A J_B}{J_{AB}} = 1 - 2\rho \quad (25)$$

where  $\rho$  is exactly the same as defined in (15). As announced in Section 2,  $J_4$  drops out of the visibility: to the leading order in  $I$ , the loss of visibility is independent of the coherence of the four-photon state.

Since  $\rho$  is basically the probability per pulse (so that  $2\rho$  is the probability per qubit [14]) of creating a detectable pair, it defines the detection rate up to multiplicative factors. Relation (25) therefore says that, if we fix a detection rate, we shall find a given visibility, no matter whether the rate was obtained by pumping weakly and putting no filters, or by pumping strongly and putting narrow filters. This is a positive feature: filters, while being useful to improve the coherence whenever this is required, do not degrade the visibility.

As described in section 4,  $\rho$  can be measured independently, the relation (25) can be experimentally tested. This is the object of the next Section.

## 6 Experimental verification

In this section, we present an experimental verification of Eq. (25). Two-photon interference fringes are recorded for different value of  $\rho$ , corresponding to different values of pump power, with the Franson setup described in the previous Section. Let us remind the reader that the down-converted photons are at the two telecom wavelengths, 1310 nm and 1550 nm. The measurement are reported for two different filters configurations; in both cases, the larger filter is on the photons at 1550nm, so this is "mode  $b$ ".

In the first configuration, only the photon at 1310 nm is filtered with 40 nm FWHM. These data are taken from [6]. In the second configuration, both photon are filtered. The photon at 1310 nm is filtered with 10 nm FWHM, while the photon at 1550 nm is filtered with 18 nm FWHM. The coefficient  $\rho$  is measured using the side peaks method explained in Section 4. The visibility for the two experimental configurations is plotted as a function of  $2\rho$  in Fig. 4. The error bars on the experimental points represent the accuracy of the fit of the recorded interference patterns with a sine law [22]. The two solid lines are straight lines with slope  $-1$ , according to Eq. (25); the small shift between the two curves is due to the fact that the maximal visibility was not the same for both experiments and was left free as a fitting parameter. We observe a good agreement between theory and experiment. These results confirm that the loss of visibility due to four-photon events is directly related to  $\rho$ , regardless of the filtering that is applied on the photons and regardless of the coherence of the four-photon component [9]. This is therefore a general result very useful to estimate the effect of multi-pair creation in an experiment in a very simple way.

## 7 Conclusion

In summary, we have found a quantitative prediction for the loss of two-photon interference visibility due to the presence of a four-photon component in the down-converted field. The loss of visibility (25) is determined by the parameter  $\rho$  (15), that is close to the probability of creating a detectable pair. This parameter can be measured independently, thus allowing a direct experimental verification of our prediction. While the full calculation was worked out for time-bin entanglement, we have presented in Section 2 a simplified derivation that gives the same result and applies to any form of entanglement generated by down-conversion.

We acknowledge fruitful discussions with Antonio Acín, Christoph Simon and Wolfgang Tittel.

*Note added in proof.* Since this work was finished, we have learnt of two independent papers [23, 24] that discussed the loss of visibility of two-photon interferences due to the presence of higher-photon-number components. Both calculations concern entanglement in polarization and have been done in the single-mode formalism: this allows to take into account the contribution of all more-photon terms and not only of the four-photon one. The results are compatible with ours in the regime where they can be compared (small pump power). Consider for instance Ref. [24]: from their eq. (2), we see that the probability per qubit of

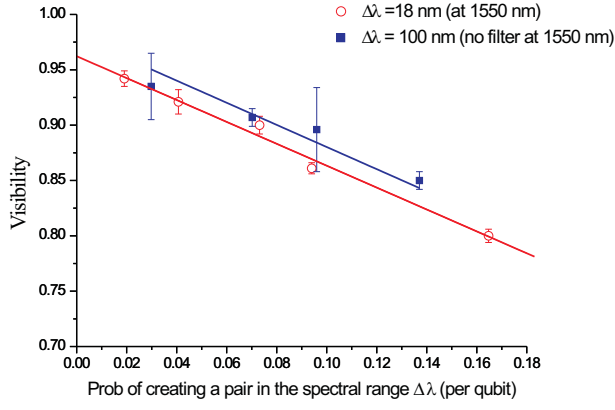


Figure 4: Visibility as a function of  $2\rho$  for two different filtering configurations. Full squares are experimental points with a 40 nm filter at 1310 nm and no filter at 1550 nm (data taken from [6]). Open circles are experimental points with a 10 nm filter at 1310 nm and a 18 nm filter at 1550 nm. The solid curves are straight line with a slope  $-1$ , according to Eq. (25).

producing a pair is  $2 \tanh^2 \tau / \cosh^4 \tau \approx 2\tau^2$ . Then our formula (3) predicts  $V \approx 1 - 2\tau^2$  for small values of  $\tau$ , which indeed fits correctly the curve of Fig. 5 of Ref. [24] up to  $\tau \approx 0.5$ .

## A Appendix

We recall the definitions of  $R_2$  and  $R_4$ , formulae (19) and (20). Although we introduced them only in Section 5, the same quantities can be defined for the setup of Section 4, and in fact for any setup: a given setup will be characterized by the relation between the preparation modes  $a, b$ , and the detection modes  $a_1, b_1$ , a relation encoded in the operator  $\hat{\mathcal{A}}^\dagger$ . In this appendix, we start by working out more explicitly the general formulae for  $R_2$  and  $R_4$ ; we subsequently describe the strategy that allows a simplification of these formulae (a strategy already introduced in Ref. [9]), and finally compute the explicit results announced in Sections 4 and 5.

### A.1 General formula for $R_2$

The calculation of  $R_2$  goes as follows. The commutation rules between the input modes  $a, b$  and the detected modes  $a_1, b_1$  read

$$a_1(\nu_a) \hat{a}^\dagger(\omega_a) = \hat{a}^\dagger(\omega_a) a_1(\nu_a) + E(\omega_a, \alpha) \delta(\omega_a - \nu_a) \mathbb{1} \quad (26)$$

$$b_1(\nu_b) \hat{b}^\dagger(\omega_b) = \hat{b}^\dagger(\omega_b) b_1(\nu_b) + E(\omega_b, \beta) \delta(\omega_b - \nu_b) \mathbb{1} \quad (27)$$

where  $E(\omega, \gamma)$  is a function that depends on the evolution undergone by the modes from the production to the detection — specifically,  $E(\omega, \gamma) = 1$  for the calibration setup, while  $E(\omega, \gamma) = S(\omega, \gamma)$  given in (18) for

the Franson setup. Using these commutation relations, one finds immediately  $E_{a_1}^{(+)}(t_A) E_{b_1}^{(+)}(t_B) \hat{A}^\dagger |vac\rangle = c(t_A, t_B) |vac\rangle$  where we have introduced the complex number

$$c(t_A, t_B) \equiv \int d\underline{\omega} f_A(\omega_a) f_B(\omega_b) G(\omega_a, \omega_b) E(\omega_a, \alpha) E(\omega_b, \beta) e^{-i(\omega_a t_A + \omega_b t_B)}. \quad (28)$$

Consequently,  $R_2 = I \int dt_A dt_B |c(t_A, t_B)|^2$ . The integration over  $t_A$  and  $t_B$  can be performed before the integrals over the frequencies, so finally

$$\begin{aligned} R_2(T_A, T_B) &= I \int d\underline{\omega} d\underline{\omega}' f_A(\omega_a) f_B(\omega_b) g(\omega_a, \omega_b) f_A(\omega'_a) f_B(\omega'_b) g^*(\omega'_a, \omega'_b) \\ &\quad \times \left(1 + e^{i(\omega_a + \omega_b)\tau}\right) \left(1 + e^{-i(\omega'_a + \omega'_b)\tau}\right) \mathcal{E}(\omega_a, \omega_b, \omega'_a, \omega'_b) \\ &\quad \times e^{-i(\omega_a - \omega'_a)T_A} e^{-i(\omega_b - \omega'_b)T_B} (\Delta T)^2 \text{sinc}[(\omega_a - \omega'_a)\Delta T] \text{sinc}[(\omega_b - \omega'_b)\Delta T] \end{aligned} \quad (29)$$

where we have defined the shortcut

$$\mathcal{E}(\omega_a, \omega_b, \omega'_a, \omega'_b) = E(\omega_a, \alpha) E(\omega_b, \beta) E^*(\omega'_a, \alpha) E^*(\omega'_b, \beta). \quad (30)$$

In (29), the first two lines are simply the expansion of the  $G$ 's and the evolution term  $\mathcal{E}$ ; the last line is the result of the integration over  $t_A$  and  $t_B$ .

## A.2 General formula for $R_4$

The calculation of  $R_4$  follows exactly the same structure as the calculation of  $R_2$ , only the formulae are heavier. Using

$$a_1(\nu) \hat{a}^\dagger(\omega) \hat{a}^\dagger(\omega') = \hat{a}^\dagger(\omega) \hat{a}^\dagger(\omega') a_1(\nu) + E(\omega, \alpha) \delta(\omega - \nu) \hat{a}^\dagger(\omega') + E(\omega', \alpha) \delta(\omega' - \nu) \hat{a}^\dagger(\omega) \quad (31)$$

and the analogous relation for mode  $b$ , one finds

$$E_{a_1}^{(+)}(t_A) E_{b_1}^{(+)}(t_B) (\hat{A}^\dagger)^2 |vac\rangle = |AB\rangle + |A'B'\rangle + |A'B\rangle + |AB'\rangle \equiv 2(|AB\rangle + |AB'\rangle). \quad (32)$$

We have defined

$$|AB\rangle = \int d\underline{\omega} d\underline{\omega}' G(\omega_a, \omega_b) G(\omega'_a, \omega'_b) Z(\omega_a, \omega_b, \omega'_a, \omega'_b) |vac\rangle$$

where  $Z$  is the non-normalized two-photon creation operator

$$Z(\omega_a, \omega_b, \omega'_a, \omega'_b) = f_A(\omega_a) f_B(\omega_b) e^{-i(\omega_a t_A + \omega_b t_B)} E(\omega_a, \alpha) E(\omega_b, \beta) a_1^\dagger(\omega'_a) b_1^\dagger(\omega'_b);$$

$|AB'\rangle$  is obtained from  $|AB\rangle$  by replacing  $\omega_b \leftrightarrow \omega'_b$  in  $Z$ , or equivalently by relabelling the integration variables:

$$|AB'\rangle = \int d\underline{\omega} d\underline{\omega}' G(\omega_a, \omega'_b) G(\omega'_a, \omega_b) Z(\omega_a, \omega_b, \omega'_a, \omega'_b) |vac\rangle.$$

Obviously, by simply exchanging primed and unprimed integration variables,  $|AB\rangle = |A'B'\rangle$  and  $|AB'\rangle = |A'B\rangle$ , whence the r.h.s. of (32). Inserting (32) into (20), we see that the quantity that we must compute is

$$\begin{aligned} R_4(T_A, T_B) &= I^2 \int dt_A dt_B [\langle AB|AB\rangle + (\langle AB|AB'\rangle + c.c.) + \langle AB'|AB'\rangle] \\ &= R_{4,1}(T_A, T_B) + [R_{4,2}(T_A, T_B) + c.c.] + R_{4,3}(T_A, T_B). \end{aligned} \quad (33)$$

The integrals over  $t_A$  and  $t_B$  are exactly the same ones that we had in the calculation of  $R_2$ .

The first term of the sum (33) is the easiest one, and can be given in closed form. In fact, in  $|AB\rangle$  the integrals over  $\underline{\omega}$  and  $\underline{\omega}'$  are factored, and in addition, the integral on  $\underline{\omega}$  gives the same  $c(t_A, t_B)$  that we met in the calculation of  $R_2$ , formula (28). That is,  $|AB\rangle = c(t_A, t_B) \int d\underline{\omega}' G(\omega'_a, \omega'_b) a_1^\dagger(\omega'_a) b_1^\dagger(\omega'_b) |vac\rangle$ . Consequently,  $R_{4,1}(T_A, T_B) = I R_2(T_A, T_B) \int d\underline{\omega} |G(\omega_a, \omega_b)|^2$  where we recall that  $G(\omega_a, \omega_b) = g(\omega_a, \omega_b)(1 + e^{i(\omega_a + \omega_b)\tau})$ . Anticipating over the discussion of the next subsection, we use here the fact that the terms that fluctuate in  $\tau$  average to zero; so the last integral is finally equal to  $2 \int d\underline{\omega} |g(\omega_a, \omega_b)|^2 = 2J$ . In conclusion, the first term of the sum (33) is

$$R_{4,1}(T_A, T_B) = 2 I J R_2(T_A, T_B). \quad (34)$$

The second term of the sum (33),  $R_{4,2}(T_A, T_B) = I^2 \int dt_A dt_B \langle AB|AB'\rangle$  gives

$$\begin{aligned} I^2 \int d\underline{\omega} d\underline{\omega}' d\underline{\omega}'' & f_A(\omega_a) f_A(\omega'_a) f_B(\omega_b) f_B(\omega'_b) g^*(\tilde{\omega}_a, \tilde{\omega}_b) g^*(\omega'_a, \omega'_b) g(\tilde{\omega}_a, \omega_b) g(\omega_a, \tilde{\omega}_b) \\ & \times \left(1 + e^{-i(\tilde{\omega}_a + \tilde{\omega}_b)\tau}\right) \left(1 + e^{-i(\omega'_a + \omega'_b)\tau}\right) \left(1 + e^{i(\tilde{\omega}_a + \omega_b)\tau}\right) \left(1 + e^{i(\omega_a + \tilde{\omega}_b)\tau}\right) \\ & \times \mathcal{E}(\omega_a, \omega_b, \omega'_a, \omega'_b) \\ & \times e^{-i(\omega_a - \omega'_a)\tau} e^{-i(\omega_b - \omega'_b)\tau} (\Delta T)^2 \text{sinc}[(\omega_a - \omega'_a)\Delta T] \text{sinc}[(\omega_b - \omega'_b)\Delta T]. \end{aligned} \quad (35)$$

The third term  $R_{4,3}(T_A, T_B) = I^2 \int dt_A dt_B \langle AB'|AB'\rangle$  gives

$$\begin{aligned} I^2 \int d\underline{\omega} d\underline{\omega}' d\underline{\omega}'' & f_A(\omega_a) f_A(\omega'_a) f_B(\omega_b) f_B(\omega'_b) g^*(\tilde{\omega}_a, \omega'_b) g^*(\omega'_a, \tilde{\omega}_b) g(\tilde{\omega}_a, \omega_b) g(\omega_a, \tilde{\omega}_b) \\ & \times \left(1 + e^{-i(\tilde{\omega}_a + \omega'_b)\tau}\right) \left(1 + e^{-i(\omega'_a + \tilde{\omega}_b)\tau}\right) \left(1 + e^{i(\tilde{\omega}_a + \omega_b)\tau}\right) \left(1 + e^{i(\omega_a + \tilde{\omega}_b)\tau}\right) \\ & \times \mathcal{E}(\omega_a, \omega_b, \omega'_a, \omega'_b) \\ & \times e^{-i(\omega_a - \omega'_a)\tau} e^{-i(\omega_b - \omega'_b)\tau} (\Delta T)^2 \text{sinc}[(\omega_a - \omega'_a)\Delta T] \text{sinc}[(\omega_b - \omega'_b)\Delta T]. \end{aligned} \quad (36)$$

Note that, as it should, the difference between  $R_{4,2}(T_A, T_B)$  and  $R_{4,3}(T_A, T_B)$  is only in the contribution of the  $G$ 's, lines one and two.

### A.3 Strategy of the calculation

One cannot go beyond the formulae that we just derived for  $R_2$  and  $R_4$  without specifying what the evolution  $\mathcal{E}(\omega_a, \omega_b, \omega'_a, \omega'_b)$  is (that is, without specifying the setup) and without a simplification strategy. Here is how this strategy goes [9].

1. We first notice that the times  $T_A, T_B$  of interest are typically 0,  $\tau$  etc; and as we said,  $\mathcal{E}(\omega_a, \omega_b, \omega'_a, \omega'_b)$  is also a product of terms containing either 1 or some  $e^{i\omega\tau}$ . So all our integrals for  $R_2$  and  $R_4$  are in fact sums of integrals of the form  $\int d\underline{\omega} \mathcal{F}(\underline{\omega}) e^{i\Omega(\underline{\omega})\tau}$ . Here,  $\mathcal{F}$  is a product of  $g(\omega, \omega')$ 's (spectral function of the pump and phase matching conditions) and of cardinal sines  $\text{sinc}((\omega - \omega')\Delta T)$  associated to the time-resolution of the detectors;  $\Omega$  is an algebraic sum of the some of the integration variables  $\underline{\omega}$ .
2. Because we want the two pump pulses to be well-separated (well-defined time-bins), it turns out that all the integrals in which  $\Omega \neq 0$  will average to zero. In fact, the typical width of  $g$  is  $\frac{1}{t_c^{pump}} \geq \frac{1}{\Delta t}$ ,

where  $t_c^{ump}$  and  $\Delta t$  are, respectively, the coherence time and the temporal width of each pump pulse  $p(t)$ . If the time-bins are to be well-defined, we must impose  $\tau \gg \Delta t$ . Moreover, if one wants to distinguish the time-bins at detection, one must also have a sufficiently small time-resolution for the detector; so  $\tau \gg \Delta T$ . In summary: in the frequency domain (which is the integration domain), if  $\Omega \neq 0$  the term  $e^{i\Omega(\underline{\omega})\tau}$  fluctuates with period  $\frac{1}{\tau}$ , while in this range  $\mathcal{F}(\underline{\omega})$  is almost constant. The second step of the calculation consists then in going through the factors to sort out those integrals in which  $\Omega = 0$ . This is the clever trick that allows one to obtain readable formulae.

3. This being done, one can also perform the limit  $\Delta T \rightarrow \infty$ , leading to  $\text{sinc}(x\Delta T) \simeq \frac{1}{\Delta T}\delta(x)$ . In fact,  $x$  is of the form  $\omega - \omega'$ , and this is in average close to the spectral width of each down-converted photon  $\frac{1}{t_c^{ph}}$ . But a detector cannot detect a photon unless  $\Delta T \gg t_c^{ph}$ . This is the precise meaning of the formal limit  $\Delta T \rightarrow \infty$ . Obviously this limit must be performed *after* the estimate described in point 2.

In summary, for each of the setups that we want to study, we must replace  $\mathcal{E}(\omega_a, \omega_b, \omega'_a, \omega'_b)$  with its explicit value, then by inspection identify those terms for which the dependance in  $\tau$  identically vanishes under the integral.

## A.4 Calculations for section 4

For the calibration setup of section 4, we must compute  $R(0, 0)$  and  $R(\tau, 0)$ . Here,  $\mathcal{E}(\omega_a, \omega_b, \omega'_a, \omega'_b) = 1$  because the modes don't evolve from the preparation to the detection. Then,  $R_2$  given in (29) is the sum of four integrals because of the product in line two; while  $R_{4,2}$  and  $R_{4,3}$  given respectively by (35) and (36) are the sum of sixteen integrals because of the products in line two.

Let's set  $T_A = T_B = 0$ , and look first at  $R_2$ . Only the product  $1 \times 1$  gives an integral whose argument does not contain  $\tau$ , so we forget about the three other integrals. Through the limit  $\text{sinc}(x\Delta T) \simeq \frac{1}{\Delta T}\delta(x)$ , we obtain  $\omega_j = \omega'_j$  and consequently  $R_2(0, 0) = I J_{AB}$ . So we have obtained  $R(0, 0) = I J_{AB} + O(I^2)$  as announced.

If we set  $T_A = \tau$ ,  $T_B = 0$ , it is easy to become convinced that none of the four integrals that compose  $R_2$  can become independent of  $\tau$ ; therefore,  $R_2(\tau, 0) = 0$  and we must compute  $R(\tau, 0) = R_4(\tau, 0)$ . Obviously,  $R_{4,1}(\tau, 0) = 0$  because it is proportional to  $R_2$ . By inspection, one sees that  $R_{4,2}(\tau, 0) = 0$  as well since none of the sixteen integrals can be made independent of  $\tau$ . In  $R_{4,3}(\tau, 0)$ , only the integral associated to the product  $1e1e$  (with obvious notations) is independent of  $\tau$ . For this integral, we can again set  $\omega_j = \omega'_j$  and we obtain finally  $R(\tau, 0) = R_{4,3}(\tau, 0) = I^2 J_A J_B$  as announced.

## A.5 Calculation for section 5

For the Franson interferometer of section 4, we must compute  $R(\tau, \tau)$ . Here however,

$$\mathcal{E}(\omega_a, \omega_b, \omega'_a, \omega'_b) = \left(1 - e^{i(\omega_a \tau + \alpha)}\right) \left(1 - e^{i(\omega_b \tau + \beta)}\right) \left(1 - e^{-i(\omega'_a \tau + \alpha)}\right) \left(1 - e^{-i(\omega'_b \tau + \beta)}\right), \quad (37)$$

where we dropped a global factor  $\frac{1}{2^4}$ . Consequently,  $R_2$  given in (29) is the sum of  $2^6 = 64$  integrals, while  $R_{4,2}$  and  $R_{4,3}$  given respectively by (35) and (36) are the sum of  $2^8 = 256$  integrals.

Let's look at  $R_2$ . By inspection, one finds that the integrals whose argument is independent of  $\tau$  are four:  $ee|1111$ , that gives a contribution 1;  $11|eeee$ , that also gives a contribution 1;  $1e|ee11$ , whose contribution is  $e^{i(\alpha+\beta)}$ ; and  $e1|11ee$ , whose contribution is  $e^{-i(\alpha+\beta)}$ . In these notations, the first two items correspond to the products of terms of line two, the last four items correspond to the products within  $\mathcal{E}$ . Finally, performing the limit  $\Delta T \rightarrow \infty$  we find

$$R_2(\tau, \tau) = 2 I J_{AB} (1 + \cos(\alpha + \beta)) \quad (38)$$

that is indeed (21) up to a multiplicative factor 2. Immediately then we have also

$$R_{4,1}(\tau, \tau) = 4 I^2 J_{AB} (1 + \cos(\alpha + \beta)) \quad (39)$$

accounting for the first term of the r.h.s. of (22).

Moving to  $R_{4,2}$ , by inspection, one can verify that the only integrals that will not average to zero are those associated to the following four products:  $1111|eeee$  and  $eeee|1111$ , both giving 1;  $1e11|ee11$ , that gives  $e^{i(\alpha+\beta)}$ ; and  $e1ee|11ee$ , that gives  $e^{-i(\alpha+\beta)}$ . As before, in these notations the first four items represent the terms of line two of (35), the last four items correspond to the products within  $\mathcal{E}$ . After the usual limit, one finds

$$R_{4,2}(\tau, \tau) + c.c = 2 I^2 J_4 (1 + \cos(\alpha + \beta)) \quad (40)$$

accounting for the second term on the r.h.s. of (22).

As for  $R_{4,3}$ , again only four integrals out of 256 will not average to zero, namely those associated to  $1111|eeee$ ,  $eeee|1111$ ,  $1e1e|e1e1$  and  $e1e1|1e1e$ ; however here, all these contributions give simply 1, so finally

$$R_{4,3}(\tau, \tau) = 4 I^2 J_A J_B \quad (41)$$

that is the last term in the r.h.s. of (22). This concludes our demonstration.

## References

- [1] D. Bouwmeester, A. Ekert, A. Zeilinger (eds), The Physics of Quantum Information (Springer, Berlin, 2000)
- [2] W. Tittel, G. Weihs, Quant. Inf. Comp. **2**, 3 (2001)
- [3] L. Mandel, E. Wolf, Optical Coherence and Quantum Optics (Cambridge University Press, Cambridge, 1995), chap. 22.4
- [4] D.F. Walls, G.J. Milburn, Quantum Optics (Springer Verlag, Berlin, 1994), chap. 5.
- [5] C. Simon, D. Bouwmeester, Phys. Rev. Lett. **91**, 053601 (2003)

- [6] I. Marcikic, H. de Riedmatten, W. Tittel, V. Scarani, N. Gisin, H. Zbinden, Phys. Rev. A **66**, 062308 (2002)
- [7] H. Weinfurter, M. Żukowski, Phys. Rev. A **64**, 010102 (2001)
- [8] P.R. Tapster, J.G. Rarity, J. Mod. Opt. **45**, 595 (1998)
- [9] H. de Riedmatten, V. Scarani, I. Marcikic, A. Acín, W. Tittel, H. Zbinden, N. Gisin, J. Mod. Opt. **51**, 1637 (2004)
- [10] K. Tsujino, H. Hofmann, S. Takeuchi, K. Sasaki, Phys. Rev. Lett. **92**, 153602 (2004)
- [11] I. Marcikic, H. de Riedmatten, W. Tittel, H. Zbinden, M. Legré, N. Gisin, quant-ph/0404124
- [12] W. Tittel, J. Brendel, H. Zbinden, N. Gisin, Phys. Rev. Lett. **84**, 4737 (2000)
- [13] I. Marcikic, H. de Riedmatten, W. Tittel, H. Zbinden, N. Gisin, Nature **421**, 509 (2003); H. de Riedmatten, I. Marcikic, W. Tittel, H. Zbinden, D. Collins, N. Gisin, Phys. Rev. Lett. **92**, 047904 (2004)
- [14] In Sections 3-6 of this paper, where we focus on time-bin entanglement, we call "pulse" each pulse that enters the non-linear crystal; therefore, one qubit is created by two pulses. In Ref. [6], we had used "pulse" to describe each pulse produced by the pump laser, each such process creating a qubit. So "per pulse" in Ref. [6] is equivalent to "per qubit" here.
- [15] T.E. Keller, M.H. Rubin, Phys. Rev. A **56**, 1534 (1997)
- [16] W.P. Grice, I.A. Walmsley, Phys. Rev. A **56**, 1627 (1997)
- [17] Z.Y. Ou, J.-K. Rhee, L.J. Wang, Phys. Rev. A **60**, 593 (1999).
- [18] This efficiency factor takes into account the losses on the lines, the quantum efficiency  $\eta$  of the detector, and the amplitude of each monochromatic field component (whose weak  $\nu$ -dependance has been omitted).
- [19] J. D. Franson, Phys. Rev. Lett. **62**, 2205 (1989); reviewed in: M.O. Scully, M.S. Zubairy, Quantum Optics (Cambridge Univ. Press, 1997), p. 597.
- [20] Rigorously,  $\theta = \varepsilon \omega$ . However, since we have extracted the main contribution  $\omega \tau$ , we have  $\varepsilon \Delta \omega \ll \pi$ , with  $\Delta \omega$  the spectral width of the photons ( $\Delta_{A,B}$ ). Consequently, we set  $\theta = \varepsilon \bar{\omega}$  with  $\bar{\omega}$  the central frequency of the photon.
- [21] Again, we give coincidence rates up to global multiplicative factors. In particular, the multiplicative factor omitted in Section 4 is not the same as the one omitted here: as can be found in the appendix, to compare the rates in the two Sections, the rates presented in this Section must be multiplied by  $\frac{1}{8}$ . This factor is indeed what one expects, because suppose that  $R_c$  is the rate of detection of a pair in the setup of Section 4. For the Franson interferometer, in only  $\frac{1}{4}$  of the cases both photons will arrive in the intermediate time-bin, and there are four possible detection patterns; but the energy available



to create a pair is the energy of two pulses; so indeed the detection rate (averaged over all choices of  $\alpha + \beta$ ) in the Franson setup, supposing the same losses in the lines, is  $R_F = (\frac{1}{4} \times \frac{1}{4} \times 2)R_c = \frac{1}{8}R_c$ .

[22] The data obtained in the early experiment (full squares in Fig. 4) are more noisy than the new ones (open circles) because the crystal that we used in 2001 was less efficient and because in the meantime we have improved the techniques to stabilize the interferometers.

[23] S.A. Podoshvedov, J. Noh, K. Kim, Opt. Commun. **232**, 357 (2004)

[24] H.S. Eisenberg, G. Khoury, G. Durkin, C. Simon, D. Bouwmeester, quant-ph/0408030